World Academy of Science, Engineering and Technology
International Journal of Mechanical and Materials Engineering
Vol:13, No:10, 2019

Failure Analysis of a Medium Duty Vehicle Leaf Spring

Gül Çevik

***Abstract*—**This paper summarizes the work conducted to assess the root cause of the failure of a medium commercial vehicle leaf spring failed in service. Macro- and micro-fractographic analyses by scanning electron microscope as well as material verification tests were conducted in order to understand the failure mechanisms and root cause of the failure. Findings from the fractographic analyses indicated that failure mechanism is fatigue. Crack initiation was identified to have occurred from a point on the top surface near to the front face and to the left side. Two other crack initiation points were also observed, however, these cracks did not propagate. The propagation mode of the fatigue crack revealed that the cyclic loads resulting in crack initiation and propagation were unidirectional bending. Fractographic analyses have also showed that the root cause of the fatigue crack initiation and propagation was loading the part above design stress. Material properties of the part were also verified by chemical composition analysis, microstructural analysis by optical microscopy and hardness tests.

***Keywords*—**Leaf spring, failure analysis, fatigue, fractography.

I. Introduction

LEAF springs are used as suspension system elements in automotive industry to overcome the vibrations, cyclic and impact loadings on the vehicle and road conditions of the vehicle trips. Hot rolling process is the most widely used manufacturing method as it is an efficient and low cost method [1]. During manufacturing of high strength steel leaf springs, decarburization occurs on the surface during heat treatment process by means of carbon atom removal from the steel in gaseous phase as a result of the interaction of carbon atoms at the steel surface with the furnace atmosphere [2]-[4]. High decarburization results in reduction of fatigue life and wear life of the part [2]. A decarburization layer of 0,5 to 1,0 mm was reported to reduce the fatigue life of leaf spring to less than one half of a surface polished spring [5], [6]. Shot peening has been used on leaf spring manufacturing processes to improve the fatigue life of leaf springs by means of surface hardening and formation of compressive residual stresses on the surface [7]. It is a widely used method as it is capable of increasing the operating lifetime by five to ten times or more when compared to un-peened springs and is relatively inexpensive [8].

Although many studies are conducted on the durability improvements of the leaf springs, they often suffer from catastrophic fatigue failures. Failures occur due to high cyclic loads as well as due to surface defects which act as stress raisers. Another major failure factor is the severe residual stresses created during the forming operation [8]. Thus, factors effective in durability and strength of springs; and failure analysis of springs have been the subject of research and experimental studies in literature. Examples of studies on effective parameters on final durability include optimizing surface profiles during hot rolling [9], effective factors of surface defects in hot rolling processes using multilevel regressions [10] and effect of cooling rate during manufacturing processes [11]. On the other side, failure analysis studies concentrated on the relationships between the dynamic factors effective in fatigue failure and fracture surface examinations to predict and assess the failure mechanisms of springs. Xu et al. conducted experimental investigations by pulsating bending tests to evaluate the effect of residual stresses on the fracture topography [12]. Sustarsic et al. studied the fatigue strength of mono- and double-leaf springs of 51CrV4 steel; in different loading modes for two different heat treatment conditions and two directions of segregations of alloying elements; in relation with microstructural characterization and fractographic examinations to predict fatigue life of spring steels using the local stress gradient concept [13]. Clarke and Borowski assess fracture origin during accident sequence of a rear leaf spring in a sport utility vehicle by means of fracture surface analysis and residual-strength estimates [14].

This paper summarizes the work done to assess the root cause of a medium duty vehicle leaf spring failure. History given on the part is; the safety factors calculated by computer aided stress analysis were at acceptable levels and part passed the part durability tests; but it has failed in service. The failed spring is a high strength double leaf spring. Within the frame of this work, material verification tests and fractographic analysis were conducted to give the answer to the main question whether the part failed due to a metallurgical defect or using the part above the designed stress conditions.

II. As-Received Condition of the Part

Location of failure is shown on Fig. 1. A complete separation of the upper leaf spring has occurred on vehicle due to fracture. Failure has occurred near to the center to the front side of the leaf. Red rectangles on the picture show the material verification test sample locations.

Fracture surface conditions are shown as-received on Fig. 2. Surfaces were corroded at field. However, radial beach marks which are indications of fatigue could still easily be detected.

G.Ç. is with Ford Otomotiv Sanayi A.Ş., 34885, İstanbul, Turkey (phone: +902166649134; e-mail: gcevik@ford.com).

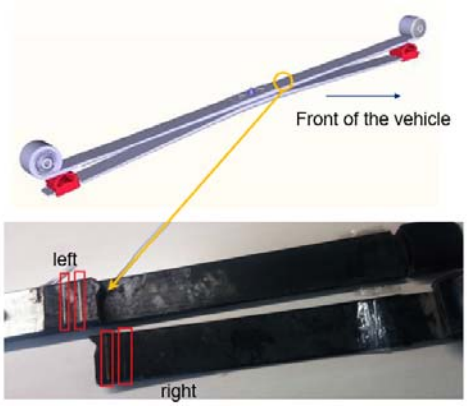

Fig. 1 Failure location

Fig. 2 Fracture surfaces at as-received condition

III. Procedure

After examining the failed part by unaided eye, material verification tests and fracture surface analyses were applied on the failed part in order to understand the failure mechanism(s), metallurgical effects and derive the root cause(s) of the failure.

A. Material Verification Tests

Based on the specified material properties of the part, material characterization tests were applied on the samples from the failed part. Namely, microstructural analysis, hardness tests and spectrometric analysis were conducted on samples.

B. Fracture Surface Analysis

Failed parts were firstly examined macroscopically to obtain initial information on the fracture surface. Following this, fracture surface examinations, fractographic analysis by Scanning Electron Microscope (SEM) were conducted to have information on the failure mechanism and any potential surface irregularities or metallurgical defects on the failed part.

IV. Material Verification Tests

The leaf spring material is a hot rolled high strength steel, 51CrV4 and used in quenched and tempered condition for this application. A shot peeing process was also applied on the part to improve the surface hardness and fatigue strength of the part.

A. Chemical Composition

To detect any possible chemical composition deviation from the specified limits of 51CrV4 steel grade, spectrometric analyses were carried out by optical emission spectrometry. No deviations from the limits were observed. Chemical composition was observed to be as specified. The specified limits of chemical composition of the part and measured values 5 mm to the failed section are shown on Table I.

TABLE I
CHEMICAL COMPOSITION LIMITS AND MEASURED VALUES

Element	Specified Limits (%)	Measured (%)
Carbon	0.14-0.55	0.5
Silicon	0.4 max	0.21
Manganese	0.70-1.1	0.83
Phosphorus	0.25 max	0.007
Sulfur	0.25 max	0.005
Chromium	0.9-1.2	0.92
Molybdenum	0.10 max	0.026
Vanadium	0.10-0.25	0.15
Nickel	0.4 max	0.11

B. Hardness

For mechanical properties aspects, hardness tests were conducted on the part from the surface to the core and compared with specified limits. The surface hardness limit is 48-56HRC and core hardness limit is 444-495HB. The measured hardness values are summarized on Table II. The hardness measurements were conducted at 5 mm and 50 mm to the failed section.

TABLE II
HARDNESS TEST RESULTS

Distance from the Surface (mm)	X-Section 50 mm from the Crack Region	X-Section 5mm to the Crack Region
0.1	48HRC	49HRC
0.3	51HRC	51HRC
1	52HRC	50HRC
7 (Core)	456HB	469HB

C. Microstructure

The required matrix phase of the microstructure is tempered martensite. The specified grain size is ASTM grade 6 or finer as per ASTM E112 [15].

A microscopical analysis was carried out by optical microscope on samples from 5 mm and 50 mm to the failed section. Observed microstructure is tempered martensite as specified. No remarkable bainite or retained austenite phases were observed within the structure which may reduce mechanical strength and durability of the part under cyclic loading conditions.

Measured grain size is ASTM grade 8 as per ASTM E112 Method or finer which is as required. Fig. 3 shows a representative micrograph from the examined samples.

As decarburization and the extent of it have a negative effect on fatigue strength of heat treated steels, the level of surface decarburization of the part was examined 5 mm and 50 mm to the failed section.

The specified level of decarburization depth of the part is 250 µm at maximum and partial type (Type 2). The observed decarburization type was partial and values of decarburization

depths from the examined region are within a range of 158 to 169 µm; which describes no abnormal decarburization profile of the part surface.

During microstructural studies, small size of oxidized laps is potentially formed by subsequent oxidation of laps originated during hot rolling process. These surface irregularities were further searched for at the crack origin region whether there is a link to the failure mechanism, during fractographic examinations by SEM and will be discussed on the Micro-Fractography section. Fig. 4 shows a representative micrograph from the surface showing both the decarburization depth of 158 µm and oxidized laps.

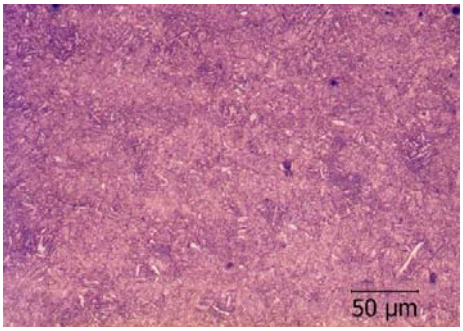

Fig. 3 Microstructure

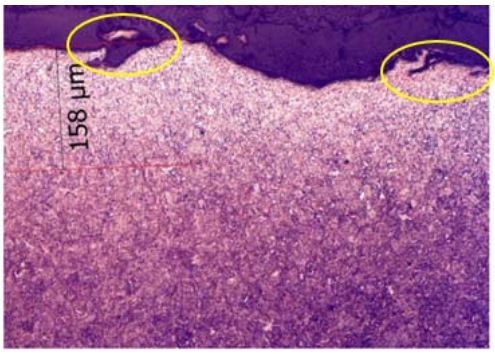

Fig. 4 Decarburization extent and surface condition

V. Fracture Surface Analysis

This section summarizes the method and results of macro- and micro-examinations conducted on the fracture surface with the aim of defining the failure mode and mechanisms and examining the section metallurgically. Microscopic examinations were conducted by SEM.

A. MacroFractography

For microscopic examinations, the surfaces were cleaned by ultrasonic cleaning method with the usage of a special cleaning agent. Left-side fracture surface after cleaning is shown on Fig. 5. The thumbnail type of fatigue crack and shear lips at the final fracture region can be differentiated on this figure.

Macro examinations showed that a fatigue crack is present on the failed section. The shear lips and rough surface to the edges describe the final fracture region. Macroscopically observable size of the fatigue crack was found to be approximately one-fourth of the total cross-sectional area. As the thumbnail shape of the crack is a possible indication of stress-corrosion cracking; further investigations were conducted on the micro-examinations and will be discussed in the micro-fractography section.

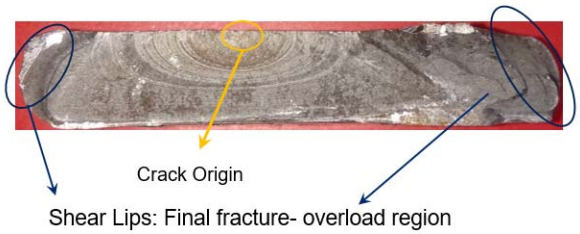

Fig. 5 Fracture surface (left-side) after ultrasonic cleaning

The orientation of the failed section and crack propagation plane describes a fatigue type of failure due to unidirectional cyclic bending loading condition.

B. Micro-fractography by SEM

Microscopic examinations were conducted to examine the crack origin, to evaluate the extent of fatigue crack with respect to complete section, to assess the root causes of the crack initiation and propagation, to examine the surface metallurgical findings on the part in microstructural analysis by optical microscopy and to define the effect of corrosion on failure.

Fig. 6 shows the locations of micro-examinations for Figs. 7-15.

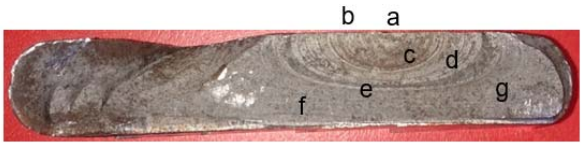

Fig. 6 Microscopic examination locations on the failed section

Fig. 7 shows the fatigue crack origin (point a) at X350 magnification. Ratchet marks which are indications of fatigue crack initiation mechanism were observed at the crack origin. Crack has emanated from a surface collapse of ~500 µm which is possibly formed by plastic deformation of the surface during shot peening process. On the other hand, this is accepted as a natural phenomenon as these regions can act as local stress-raisers.

Fig. 8 shows the extension of crack initiations further beyond to the left (point b). However these cracks did not propagate and fatigue cracking continued with initial crack starting from point a.

Examinations on crack origin showed that the crack initiation has occurred at single region. Singular crack initiation requires very low stress concentration. Examinations at crack origin region showed that this region is free of pre-existing cracks and metallurgical defects. These findings of low stress concentration and defect-free surface and singular type of crack propagation indicate that the reason of fatigue crack initiation and propagation is high magnitude of cyclic

stresses on the part.

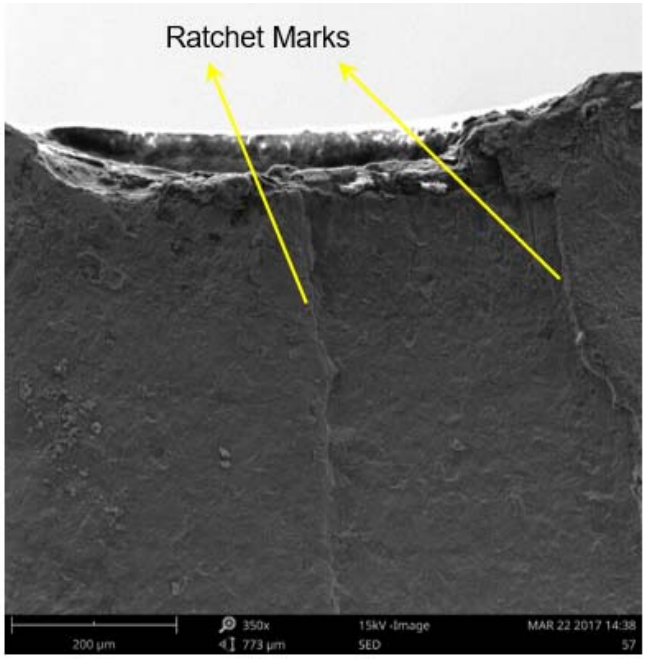

Fig. 7 Crack origin

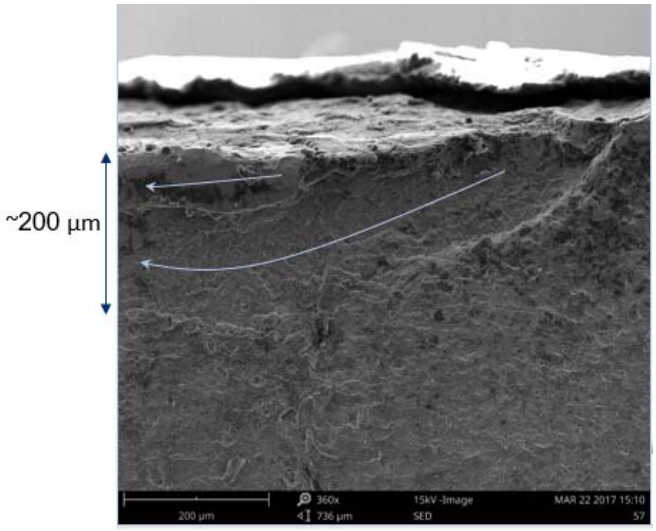

Fig. 8 Extension of multiple crack initiation

Figs. 9 and 10 show the crack propagation directions. Fatigue striations can also be observed on Fig. 9 which are indications of stable crack propagation.

Micro examinations validated that the macroscopic transition from beach marks to rough and dull surface is the transition from fatigue to final overload fracture region. Figs. 11-13 describe the replication of fracture mechanism change from fatigue to ductile failure.

Striations and tear ridges were observed in fatigue region whereas dimples were observed on the overloading region.

A ratio of 1:4 fatigue crack to final fracture region was also validated microscopically; which describes again a high stress condition on the part.

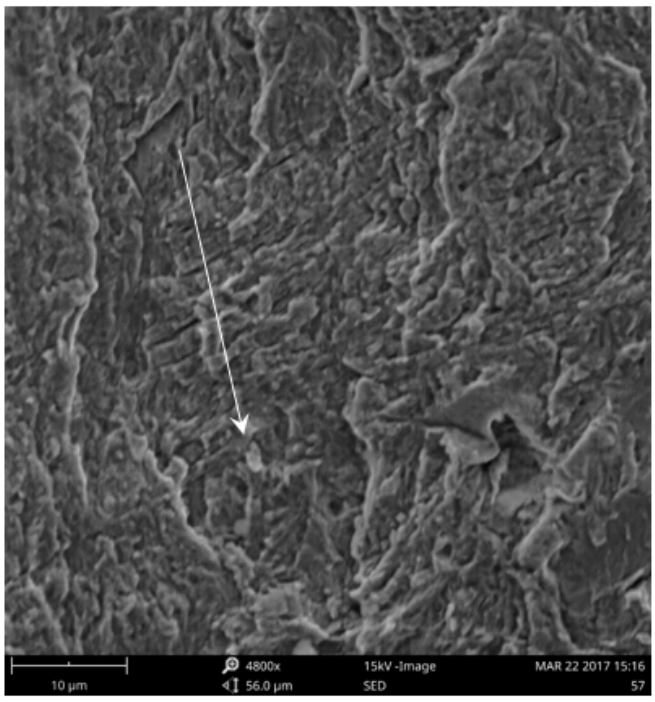

Fig. 9 Fatigue crack propagation direction and striations (point b)

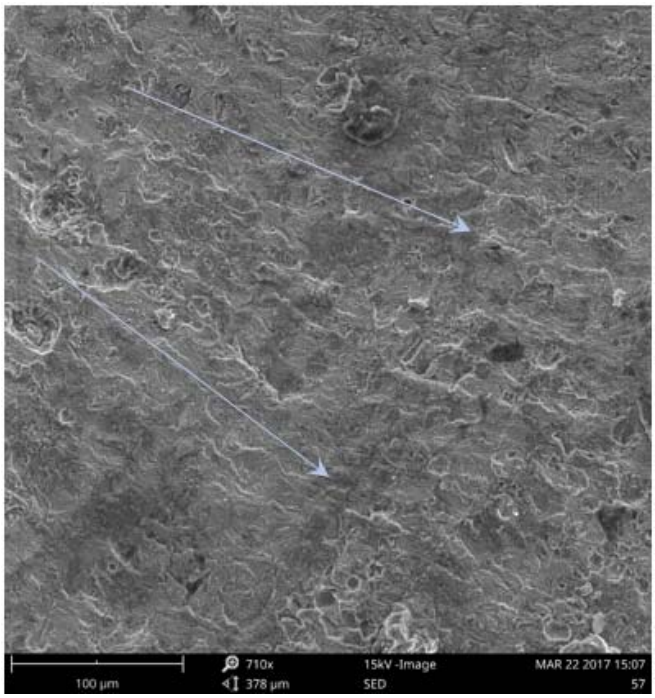

Fig. 10 Fatigue crack propagation directions (point c)

Crack initiation and propagations were also examined thoroughly in aspects of corrosion assisted crack initiation and formation; but as intergranular fracture features or localized corrosion products were not observed; which are normally indications of corrosion; there found to be no link between environmental effects and part failure.

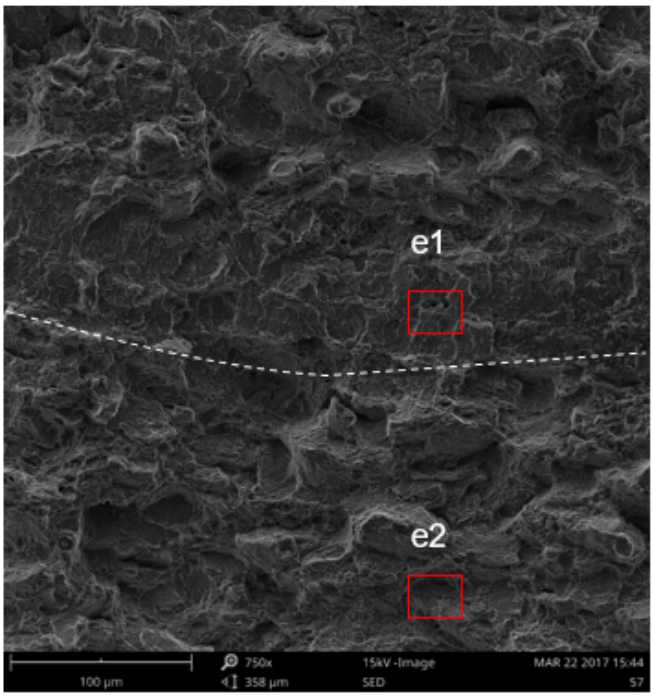

Fig. 11 Fatigue to overloading transition region (point e)

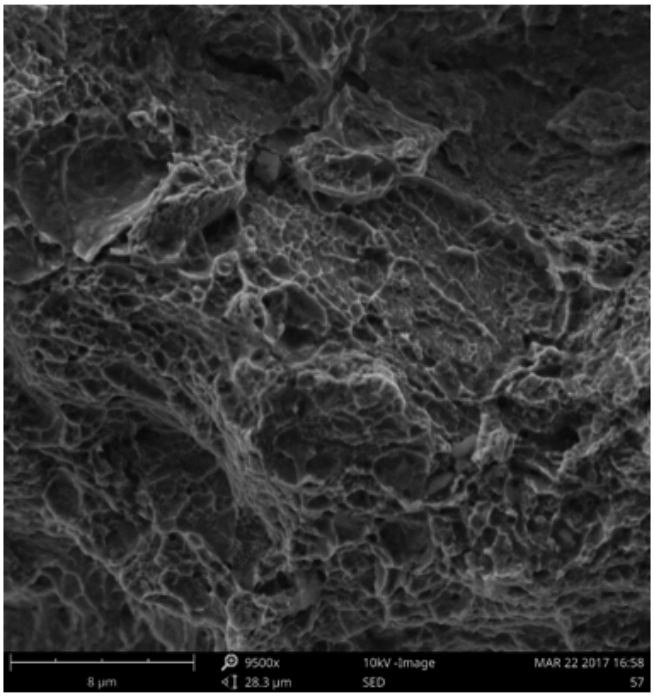

Fig. 13 Ductile dimples due to overloading failure (e2)

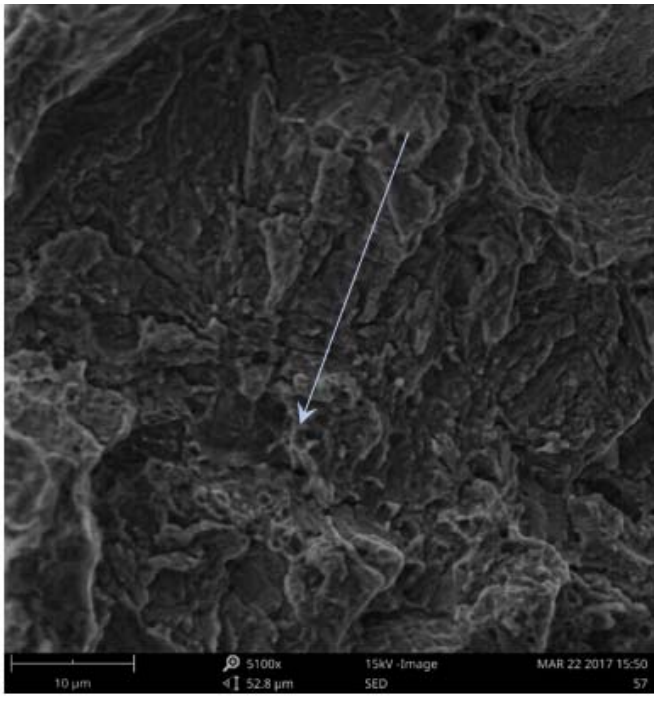

Fig. 12 Fatigue striations and tear ridges (e1)

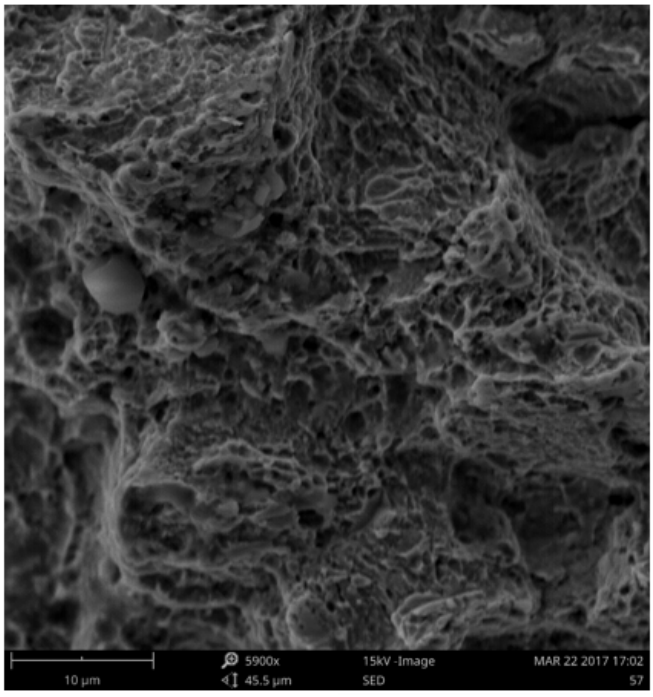

Fig. 14 Ductile dimples at final fracture (point f)

Figs. 14 and 15 show fractographs from the final failure regions. A complete ductile failure was observed near to the crack tip whereas both ductile and brittle features were observed near to the edge of the part. This may have occurred by more than one step of final overloading and increased strain rates at final stage resulting in cleavage plane formation due to brittle failure.

VI. Discussions and Conclusions

According to the failure analysis done by material verification and fractoraphic examinations within the frame of this study; following root cause assessments were done;

1) Part satisfies the defined material properties in aspects of chemical composition, mechanical properties, microstructural conditions and metallurgical integrity.

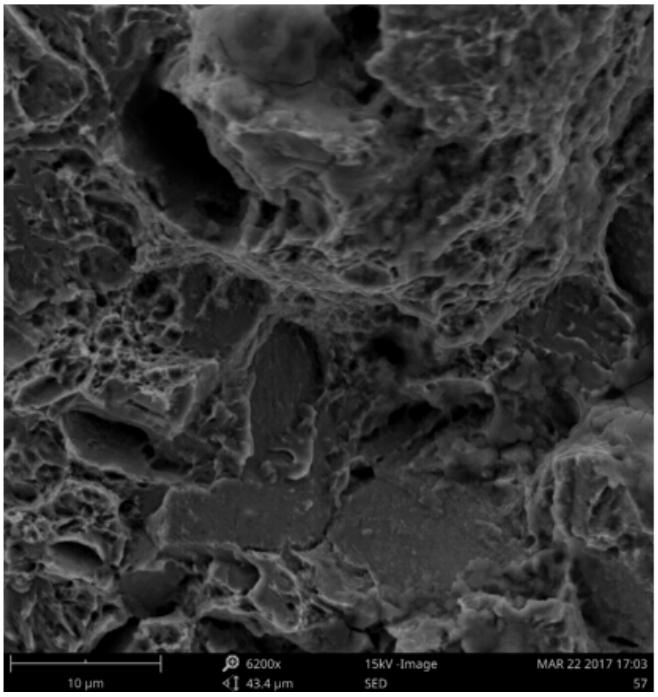

Fig. 15 Mixed type of overloading fracture (point g). Ductile dimples and brittle cleavage planes

2) Fractographic examinations showed that the mechanism of failure is fatigue crack initiation and propagation followed by final overloading fracture; due to unidirectional cyclic bending loading.
3) Singular crack propagation describes a low stress concentration on the part.
4) Crack origin was found to be free from pre-existing cracks and metallurgical defects.
5) The findings of low stress concentration; defect-free surface and singular type of crack propagation; indicate that the reason of fatigue crack initiation and propagation is high magnitude of cyclic stresses on the part.
6) The low (1:4) ratio of fatigue crack and final overloading regions also indicates that the part worked under high magnitude of cyclic stresses with respect to its fatigue strength. Thus it can be derived that the part was misused above its design stress levels.
7) Both ductile and brittle overload features were observed on the final fracture area.
8) No metallurgical defects, surface irregularities or corrosion assisted cracking was observed on the crack initiation and propagation regions. Therefore, no failure assisting mechanism is present on the failed part.

REFERENCES

[1] S. Kalpakjian and S.R. Schmid, Manufacturing Engineering and Technology, Dorling Kindersley Pvt Ltd, 2011, pp. 340-341.
[2] G.F. Vander Voort, Advanced Materials and Processes, ASM International, 2015, 127(2), pp.22-25.
[3] A. Bramley and K.F. Allen, Engineering (London), Vol 133, p 92-94, 123-126, 229-231, and 305-306, 1932.
[4] J.K. Stanley, Iron Age, Vol 151, p 31-39 and 49-55, 1943.
[5] G.A., Hamkin and M.H. Becker, Journal of Iron and Steel Institute, 125, 1931, p387.
[6] A.S. Kenneford and G.C. Ellis, Journal of Iron and Steel Institute, 164, 1950, p265.
[7] R.L. Mattson and J.G. Roberts, SAE Transactions 68, 1980, pp. 130-136.
[8] W. Koenecke, N.K. Burrell, and C. Mehelich, Metal Improvement company, Paramus NJ ,Subsidiary of Curtiss-Wright Cooperation, October 1982, Spring, Technical Article #1982016.
[9] N. Chakraborti, B. Siva Kumar, V. Satish Babu, S. Moitra, and Mukhopadhyay, Proceedings, 14th International Workshop on Computational Mechanics of Materials, 2006.
[10] N. Jin and S. Y. Zhou, Transactions of the North American Manufacturing Research Institute of SME 32, 2004.
[11] S. K. Biswas, S. J. Chen and A. Satyanarayana, Journal of Dynamical and Control Systems, vol. 7, 1997, pp. 327-340.
[12] J. Xu, D. Zhang and B. Shen, International Conference on Shot Peening-I, 1981, Paris. 1981074, pp.367-374.
[13] B. Sustarsic, P. Borkovic, W. Echlseder, G. Gerstmayr, A. Javidi and B. Sencic, Journal of Structural Integrity and Life V.11.1, 2011, pp.27-34.
[14] C.K. Clarke and G.E. Borowski, Journal of Failure Analysis and Prevention, V5(6), December 2005, pp54-63.
[15] ASTM E112-13, Standard Test Methods for Determining Average Grain Size, ASTM International, West Conshohocken, PA, 2013, www.astm.org.